

THC is being measured, and with increasing overlap the unpaired electron gets more inside the neighboring charge distribution and attracts charge density toward the nucleus where THC is being determined. This second mechanism can become competitive with the first since it is closer in to the ligand nucleus and less unpaired density is needed for a sizable contribution to the THC. Thus, a cancellation between the two mechanisms can occur, and the THC due to EP can be negative, small, or positive depending on the relative sizes of the two mechanisms. Of course, with increasing

overlap, other mechanisms such as covalency effects contribute to the THC and have to be considered.

With the MP method we have demonstrated that the negative THC observed by Gazzinelli and Micher can be explained by EP. Because of a cancellation among the indirect terms, the main contribution to the THC was shown to be the direct-exchange polarization of the ligands by the valence electron, in contrast to what was concluded earlier.³ Finally, the good agreement with experiment lends support to the accepted model⁷ of the V_K center in the alkali halides.

Color Centers in KMgF_3 †

C. R. RILEY* AND W. A. SIBLEY

Solid State Division, Oak Ridge National Laboratory, Oak Ridge, Tennessee 37830

(Received 12 November 1969)

Polarized bleaching experiments on irradiated KMgF_3 crystals show that F_2 centers absorb light at 282 and 445 nm, F_3 centers absorb at 250 and 395 nm, and V_K centers at 340 nm. The temperature dependence of the width at half maximum of the F and F_2 bands has been studied. An analysis of the F_2 -band data, assuming a linear-coupling model, indicates that the emission from this center should occur around 2.32 eV, which is close to the 2.19-eV emission observed by other workers and attributed to this center. The suppression of coloration caused by electron-trapping impurities is compared with that expected for two possible inhibition mechanisms, depending respectively on a reduced formation rate for F centers and an enhanced destruction rate of F centers. The experiments favor the latter possibility.

INTRODUCTION

APPARENTLY, only two color-center investigations of radiation damage in KMgF_3 have been made: one by Hall¹ on self-trapped holes (V_K centers) produced by x irradiation at low temperatures and the other by Hall and Leggeat² tentatively identifying F -center and F_2 -center (M -center) absorption by means of ESR and polarized luminescence experiments. KMgF_3 has the cubic perovskite structure with a lattice constant $a=3.973$ Å. In crystals of this structure the F center has D_{4h} symmetry and F_2 centers have C_{2v} symmetry. Color-center studies of this material are not only valuable in themselves, but should also prove important for future investigations of the isomorphic materials, KMnF_3 and BaTiO_3 , which are antiferromagnetic and ferroelectric, respectively.

Hall and Leggeat² suggest that a band at around 270 nm is due to F centers and one at 445 nm is due to F_2 centers. Earlier, Hall¹ proposed that a band at about 340 nm, which is present only at low temperatures, is

the result of V_K -center formation. We felt that it would be highly desirable to confirm these observations by polarized bleaching experiments on the 340- and 445-nm bands and on a band occurring at about 395 nm, which could be due to F_3 centers. Moreover, a comparison of the radiation damage properties of KMgF_3 with those of the alkali halides should be very useful. Thus, the purpose of this paper is to report on the anisotropic absorption of these bands following polarized bleaching, on the temperature dependence of the half-width of the 445- and 270-nm bands, and on the production of F and F_2 centers by high-energy electrons as a function of temperature.

EXPERIMENTAL PROCEDURE

The crystals were grown by the Stockbarger method in an argon atmosphere using purified starting material³ consisting of equal parts of MgF_2 and KF . A graphite crucible was used, and the highest temperature in the furnace was 1070°C. The growth rate was controlled at 3 mm/h. Chemical analyses were made by means of wet chemistry and mass spectroscopy. The results of these analyses are shown in Table I.

† Research sponsored by the U. S. Atomic Energy Commission under contract with Union Carbide Corp.

* Graduate Fellow from the University of Tennessee under appointment as a National Aeronautics and Space Administration Trainee.

¹ T. P. P. Hall, Brit. J. Appl. Phys. **17**, 1011 (1966).

² T. P. P. Hall and A. Leggeat, Solid State Commun. **7**, 1657 (1969).

³ We would like to thank R. B. Quincy for preparing the starting material and for some very helpful discussions.

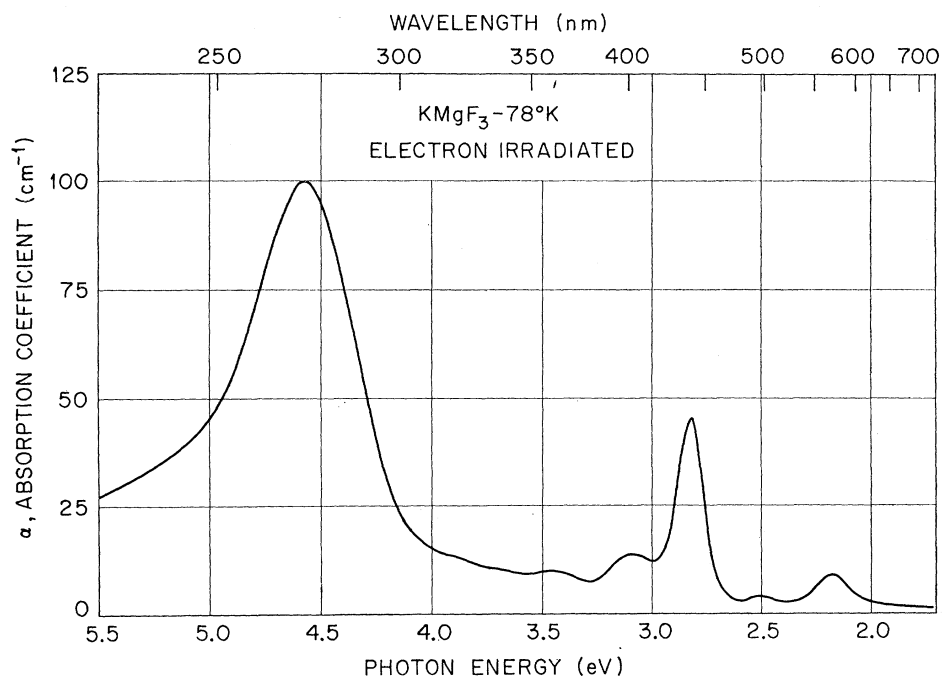


FIG. 1. Plot of the absorption coefficient versus photon energy for a 2.0-MeV electron-irradiated KMgF_3 crystal.

Samples 1 mm thick were cut from the crystal ingots with a diamond saw and were irradiated with 2.0-MeV electrons or with ^{60}Co γ rays after polishing. During electron irradiations the crystals were held in a Sulfrian liquid-helium cryostat at a fixed temperature.⁴ The temperature was monitored with a platinum resistance thermometer. Radiation intensities were measured using silver-doped phosphate glass dosimeters⁵ to be

$1.47 \times 10^{-3} \text{ MeV cm}^{-3} \text{ sec}^{-1}$ ($1.2 \times 10^{12} e \text{ cm}^{-2} \text{ sec}^{-1}$) for electron irradiations and $9 \times 10^{10} \text{ MeV cm}^{-3} \text{ sec}^{-1}$ in the case of the γ irradiations. Optical measurements were made on a Cary 14R spectrophotometer which was equipped with matched-Polaroid type HNP'B ultra-violet sheets in both the reference and the sample beams. This system transmitted light with wavelength as low as 190 nm, but the polarization was effective only to about 230 nm. Polarized bleaching was accomplished with a mercury lamp, an appropriate filter, and a Glan polarizer.

TABLE I. Impurity analysis of samples ($\mu\text{g/g}$).

| Element | Crystal | Powder |
|---------|---------|--------|
| Ag | < 1 | < 1 |
| Al | 300 | 20 |
| B | 3 | < 2 |
| Ba | < 3 | < 3 |
| Be | < 1 | < 1 |
| Bi | < 5 | < 5 |
| Ca | 30 | 20 |
| Cd | <10 | <10 |
| Co | <10 | <10 |
| Cr | < 3 | < 3 |
| Cu | < 1 | < 1 |
| Fe | 15 | 3 |
| Li | < 1 | < 1 |
| Mn | 1 | 3 |
| Mo | < 3 | < 3 |
| Na | 500 | 200 |
| Pb | < 5 | < 5 |
| Rb | 10 | 300 |
| Si | 30 | 10 |
| Sr | < 3 | < 3 |
| Ti | < 2 | < 2 |
| V | < 3 | < 3 |
| Zn | <30 | <30 |
| Zr | <10 | <10 |

⁴ W. A. Sibley and O. E. Facey, Phys. Rev. **174**, 1076 (1968).

⁵ V. H. Ritz and C. H. Cheek, Radiation Res. **25**, 537 (1965).

RESULTS

Color Centers

Figure 1 illustrates the absorption in the range 190–800 nm at 78°K from a KMgF_3 sample electron irradiated at 300°K. As mentioned previously, the bands at 270 and 445 nm have been attributed to F and F_2 centers, respectively.² The 270-nm band has a half-width W of 0.584 eV at 4°K and a peak position E_P of 4.569 eV at this temperature. At 300°K, $W=0.815$ eV and $E_P=4.488$ eV. It has been illustrated by several authors⁶ that under certain conditions $W^2(T)=W^2(0) \times \coth(\hbar\omega/2kT)$ and $W^2(0)=S(\hbar\omega)^2/8 \ln 2$, where S is the so-called Huang-Rhys factor, T is the temperature, and $\hbar\omega$ is the energy of a single phonon. From a plot of $\text{arc coth}[W^2/W(0)^2]$ versus $1/T$, illustrated in Fig. 2, we obtain $\omega=(2\pi) 6.8 \times 10^{12} \text{ sec}^{-1}$ and $S=75$.

A 254-nm optical bleach of a room-temperature irradiated crystal produced the changes in the 270-, 445-,

⁶ J. J. Markham, in *Solid State Physics*, edited by F. Seitz and D. Turnbull (Academic Press Inc., New York, 1966), Vol. 8.

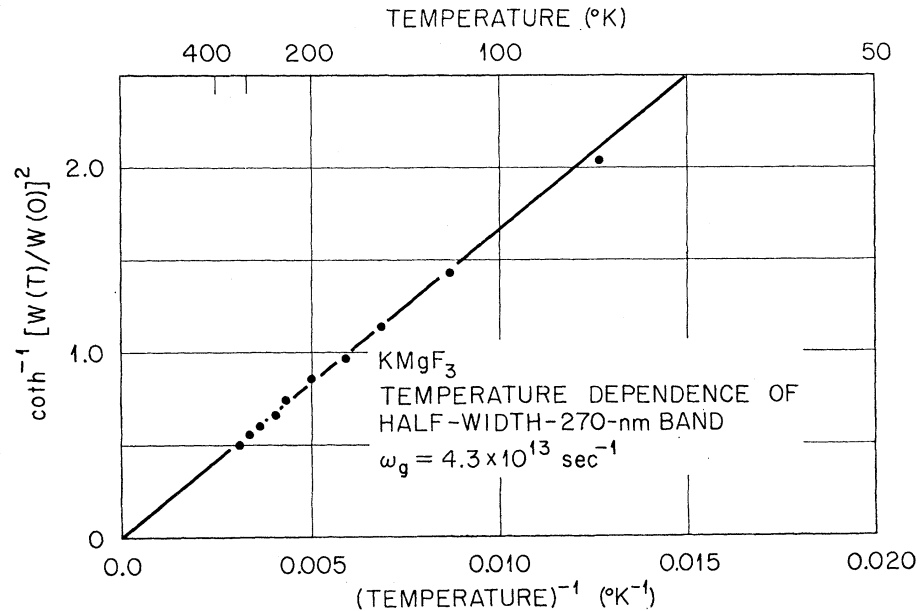


FIG. 2. Arc hyperbolic plot of the measured value of the half-width of the F band versus the reciprocal of the temperature. The frequency of the modes that broaden the F band is shown on the figure.

and 395-nm bands shown in Fig. 3. As the 270-nm band bleached out there was very little increase in the 445-nm band, but a marked increase in the 395-nm band occurred. This might suggest that the 395-nm band is due to the formation of $F_3(R)$ centers.

In cubic crystals containing anisotropic defects such as F_2 or F_3 centers, it is possible to produce macroscopic optical anisotropy by bleaching with polarized light and thus produce a preferred orientation of the centers causing the absorption.⁷⁻⁹ Two experiments are sufficient to determine whether the optical dipoles are orientated parallel to $\langle 100 \rangle$, $\langle 110 \rangle$, or $\langle 111 \rangle$ directions. The term $[110]$ light will be used to denote light with the electric vector parallel to the $[110]$ direction and

propagating in the $[001]$ direction. If anisotropies are produced in the $[110]$ and $[1\bar{1}0]$ spectra after bleaching with $[1\bar{1}0]$ light, the optical dipoles may be oriented along $\langle 110 \rangle$ or $\langle 111 \rangle$ directions but not along a $\langle 100 \rangle$ direction since $[1\bar{1}0]$ light makes equal angles with the $[100]$ and $[010]$ directions. If anisotropies are produced in the $[100]$ and $[010]$ spectra after bleaching with $[010]$ light, the optical dipoles may be oriented along $\langle 100 \rangle$ or $\langle 110 \rangle$ directions but not along a $\langle 111 \rangle$ direction since $[010]$ light makes equal angles with all $\langle 111 \rangle$ directions.

In order to confirm that the 445-nm band is due to F_2 centers, a polarized bleaching experiment was done, the results of which are shown in Fig. 4. In the top

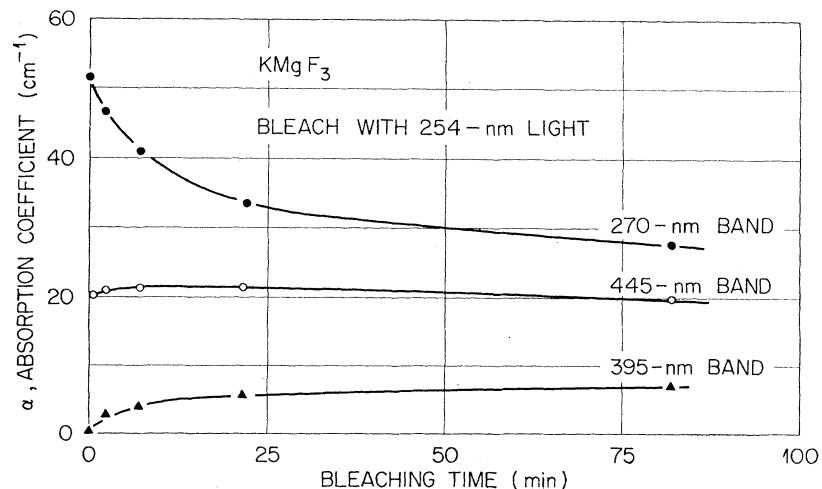


FIG. 3. Effect of 254-nm optical bleach on the 270-, 445-, and 395-nm bands.

⁷ F. Okamoto, Phys. Rev. 124, 1090 (1961).

⁸ P. P. Feofilov and A. A. Kaplyanskii, Soviet Phys.—Usp. 5, 79 (1962).

⁹ W. D. Compton and H. Rabin, Solid State Phys. 16, 121 (1964).

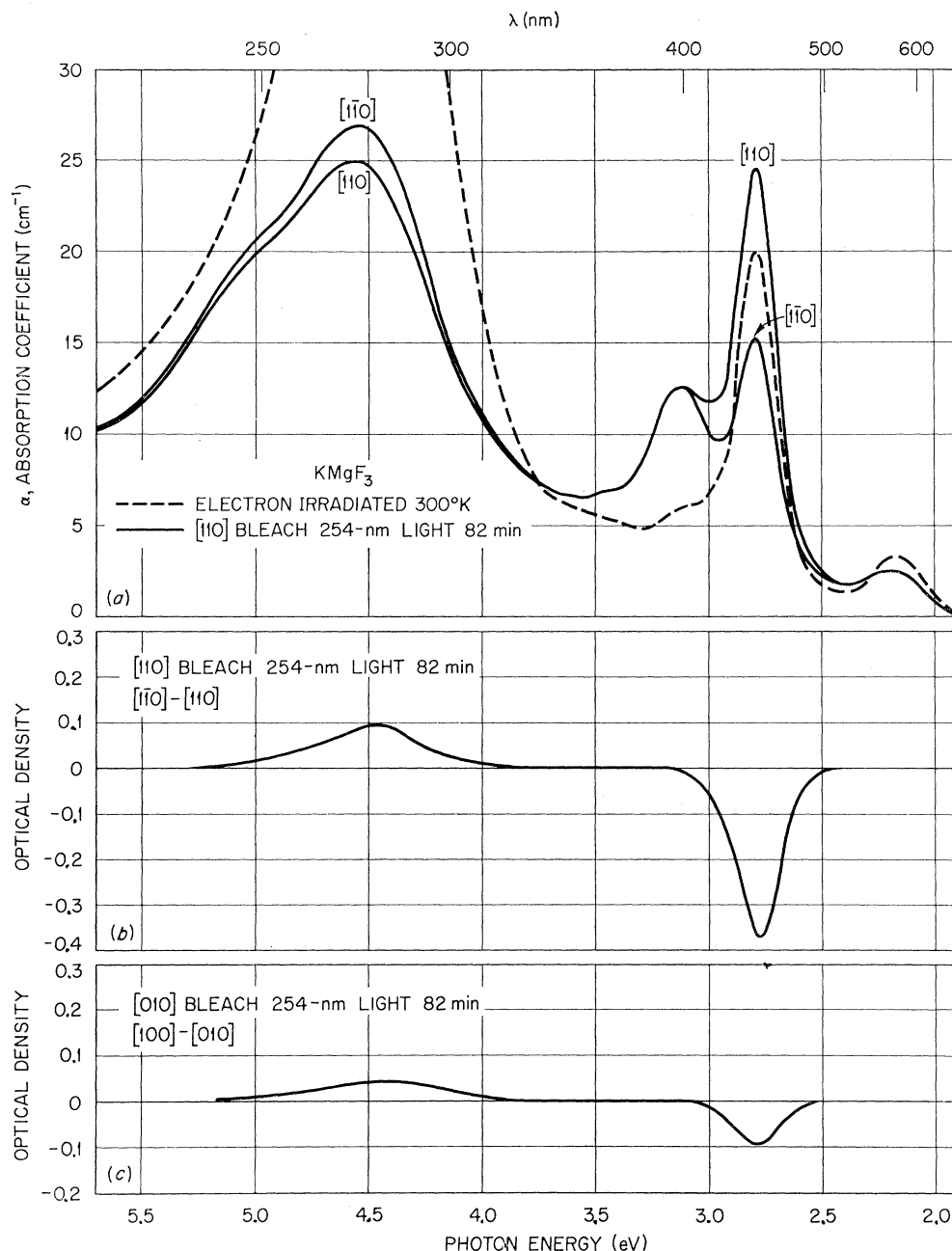


FIG. 4. Composite graph of the effect of [110] polarized 254-nm light (a) and (b) and [010] polarized 254-nm light (c) on the band at 445 nm.

panel of this figure the dashed line is the optical-absorption spectrum taken with either [110] or [110] light immediately after a 310°K electron irradiation. The two solid curves labeled [110] and [110] are the [110] and [110] spectra taken after the crystal was bleached at 300°K for 82 min with [110] 254-nm light. Note that the 395-nm band increased considerably during this bleach but is not polarized. The middle panel of the figure is the difference between the two solid lines shown in the upper panel, which is the anisotropic absorption

produced by the polarized bleach. This subtraction eliminates all bands which do not show an anisotropic absorption. Exposure to unpolarized light followed by another 310°K electron irradiation again makes the spectra isotropic and returns the bands to approximately their original heights, as in the dashed curve in the top panel. The lower panel is the difference between the [100] and [010] absorption spectra after a [010] 254-nm bleach for 82 min following the above treatment. Thus the data presented in Fig. 4 indicate that

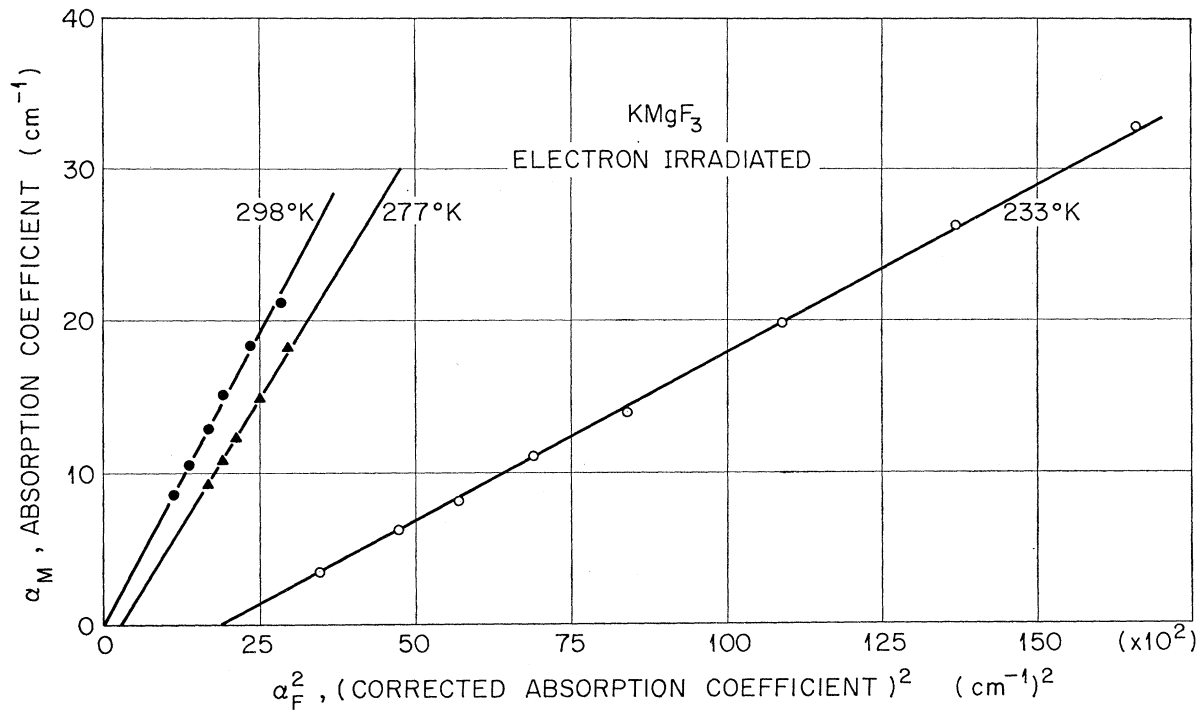


FIG. 5. Plot of the absorption coefficient at the peak of the 445-nm band versus the square of the absorption coefficient at the peak of the 270-nm band. The absorption coefficient for the 270-nm band has been corrected to account for the F_2 -center absorption which occurs in this region (see Fig. 4).

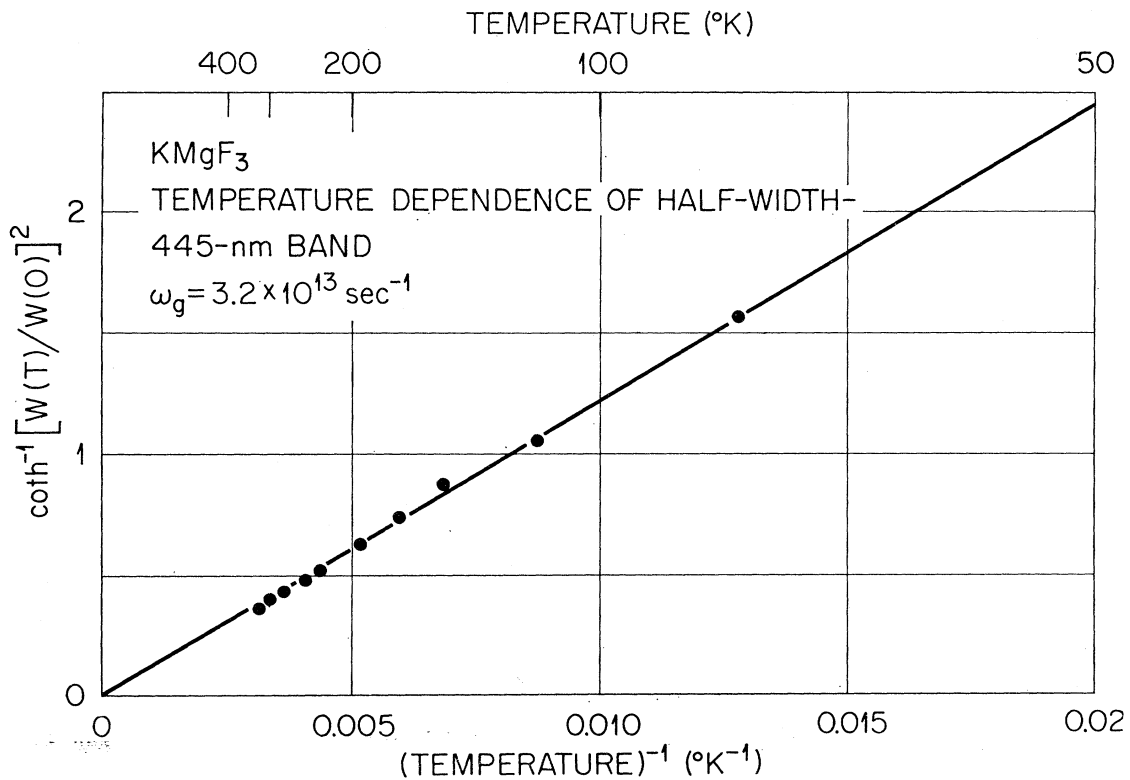


FIG. 6. Arc hyperbolic cotangent plot of the measured value of the half-width of the F_2 band versus the reciprocal of the temperature.

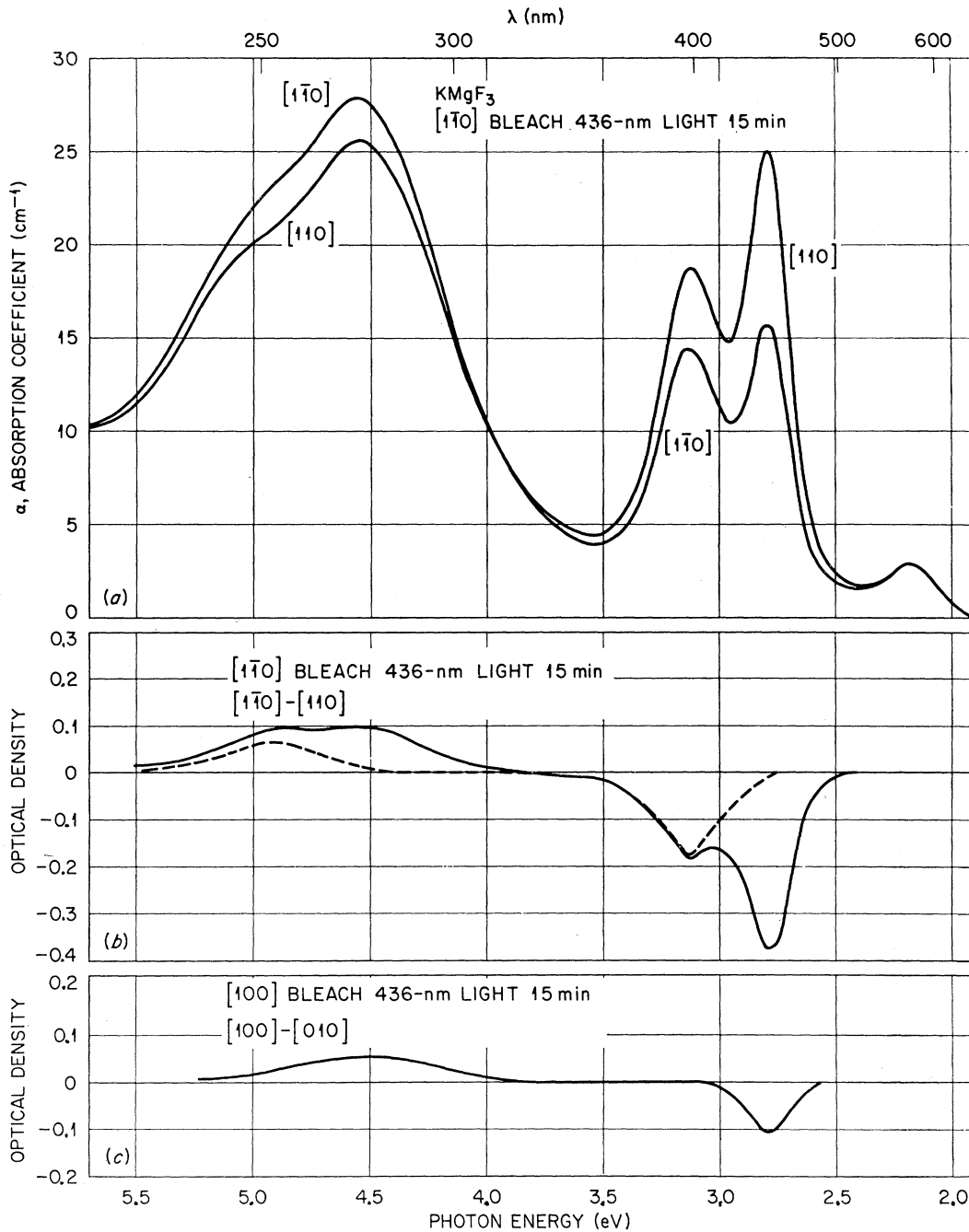


FIG. 7. Composite graph of the effect of $[1\bar{1}0]$ 436-nm light (a) and (b); and $[100]$ 436-nm light (c) on the band at 395 nm.

the 445-nm band is due to centers with their optical dipole moments oriented along $\langle 110 \rangle$ directions and is therefore most likely the F_2 band.

In alkali-halide crystals a radiation equilibrium exists between F and F_2 centers such that the concentration of F_2 centers is proportional to the square of the F -center concentration.⁹ Figure 5 is a plot of the absorption coefficient of the 445-nm band, α_M , versus the square of

the corrected absorption coefficient for the 270-nm band, α_F , for several different irradiation temperatures. From Fig. 4 it is possible to determine the amount of F_2 -center absorption under the F band. This has been subtracted from the 270-nm absorption band to give a corrected α_F in Fig. 5. The straight lines of Fig. 5 give us even more confidence that the 445-nm band is due to F_2 centers. In samples irradiated at 80°K the ratio of

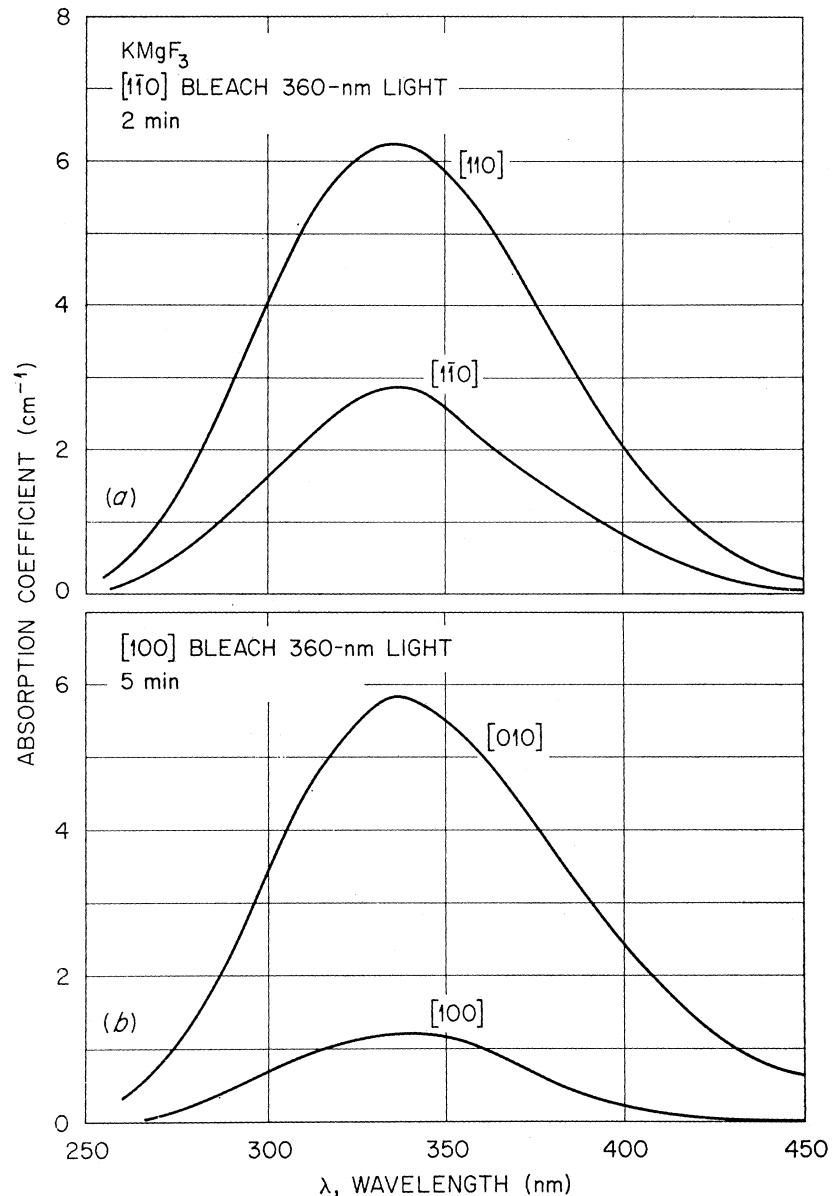


FIG. 8. Effect of $[1\bar{1}0]$ 360-nm light and $[100]$ 360-nm light on the band at 345 nm.

α_M/α_F^2 is $\sim 2.5 \times 10^{-6}$. This line would merge with the abscissa in Fig. 5 and is not shown. From this result, however, it is possible, using the equation⁹

$$\alpha_M/\alpha_F^2 = 0.87 \times 10^{17} \times (K/2N)(C_F^2/C_M)(W_F^2/W_M)(f_M/f_F^2)$$

to estimate the number of effective neighbors K necessary for F_2 -center (M -center) formation when no vacancy mobility is possible. In the equation, $N = 4.7 \times 10^{22} \text{ cm}^{-3}$ is the number of anion lattice sites, $W_F = 0.60 \text{ eV}$; $W_M = 0.15 \text{ eV}$ at 80°K , f_i is the oscillator strength, and $C_i = \mu_i(\mu_i^2 + 2)^{-2}$, where μ_i is the refractive index, so that $C_F = C_M = 0.09$. Since the ratio f_M/f_F^2 is not known, we shall consider a range of values 0.4–2.0 for this quantity. With these numbers the calculation

indicates that the effective number of neighbors K participating in the statistical production of F_2 centers in KMgF_3 ranges from 6 to 30, depending on the value chosen for f_M/f_F^2 .

The width at half-maximum of the F_2 band varies from 0.233 eV at 300°K to 0.144 eV at 4°K , and the peak position moves from 2.786 to 2.812 eV for the same temperatures. Figure 6 is a graph for the F_2 band similar to that shown in Fig. 2 for the F band. From this graph we find $\omega = (2\pi)5.1 \times 10^{12} \text{ sec}^{-1}$ and $S = 11$.

From the data in Fig. 3 there was some suggestion that the 395-nm band might be due to F_3 -center absorption. Figure 7(a) shows the $[110]$ and $[1\bar{1}0]$ spectra after a $[1\bar{1}0]$ 436-nm bleach for 15 min following the $[110]$ 254-nm bleach illustrated in Fig. 4(a). Because

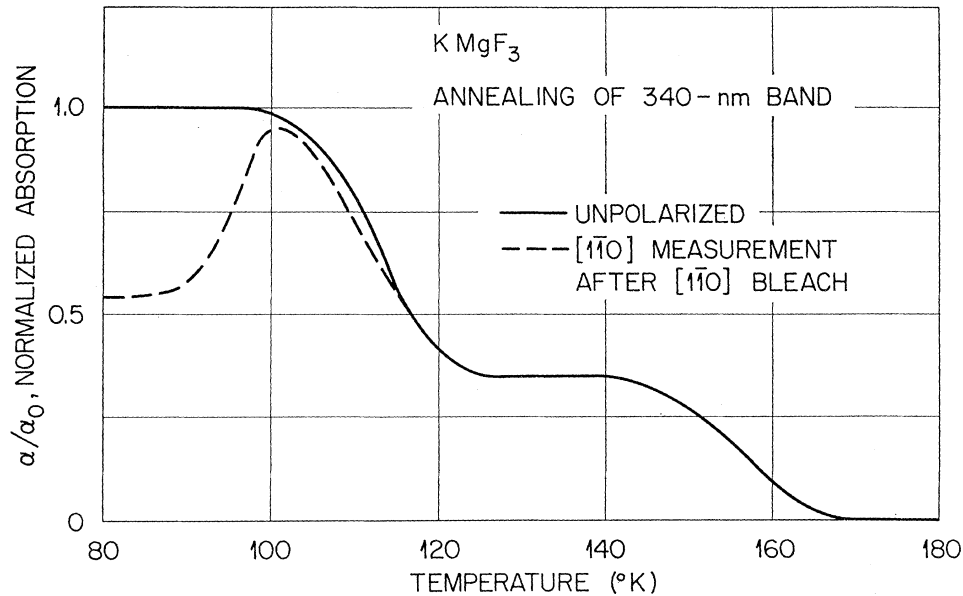


FIG. 9. Graph of the normalized absorption coefficient at the peak of the 345-nm band versus annealing temperature. The heating rate was 4°K/min and the dashed curve indicates the annealing of centers which had been previously oriented by a [110] bleach.

of the previous bleach, the F_2 centers are still oriented. The difference between the two curves in Fig. 7(a) is given in Fig. 7(b) and indicates an anisotropic absorption in addition to that due to the F_2 centers. The dashed curve in Fig. 7(b) is the result of subtracting the anisotropic absorption due to F_2 centers shown in Fig. 4(b) from that in Fig. 7(b). It should be noted that the centers responsible for the 395-nm band have another transition at about 250 nm which is oppositely polarized. Figure 7(c) shows the difference between the [100] and [010] spectra after a [100] 436-nm bleach for 15 min following the [010] bleach shown in Fig. 4(c).

In this case, the anisotropic absorption is simply that due to the previously oriented F_2 centers. Thus it appears that the 395-nm band is due to $\langle 111 \rangle$ -type centers and is most likely the F_3 band.

When a specimen is irradiated at temperatures below about 80°K, a band grows in very rapidly at 340 nm and saturates after only a small radiation dose. Polarized bleaching of this band also leads to an anisotropic absorption shown in Fig. 8 which is characteristic of centers with moments oriented along $\langle 110 \rangle$ directions. Hall¹ had previously suggested that this band might be due to V_K -center absorption. Our results are consistent

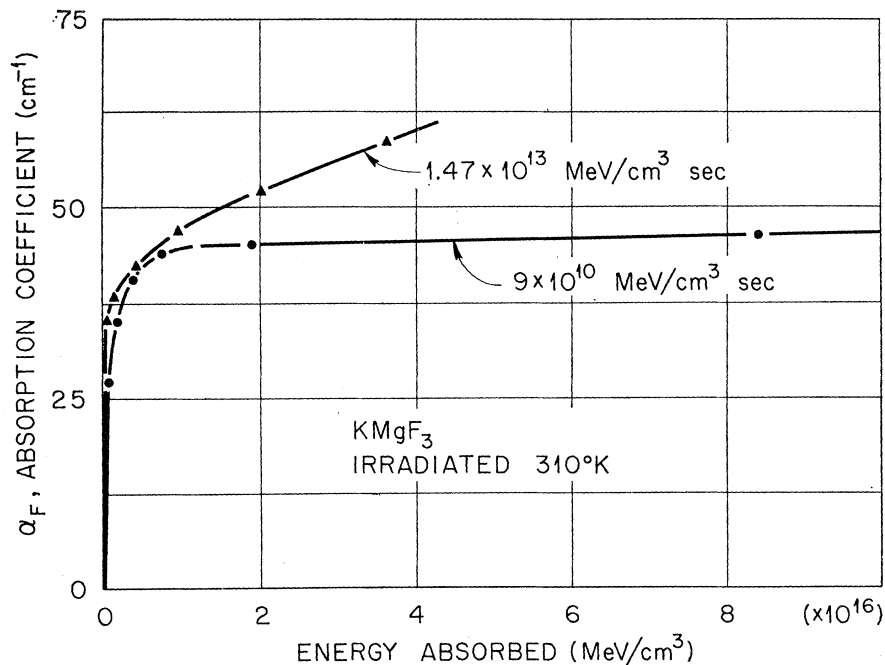


FIG. 10. Effect of radiation intensity on the room-temperature colorability of KMgF₃.

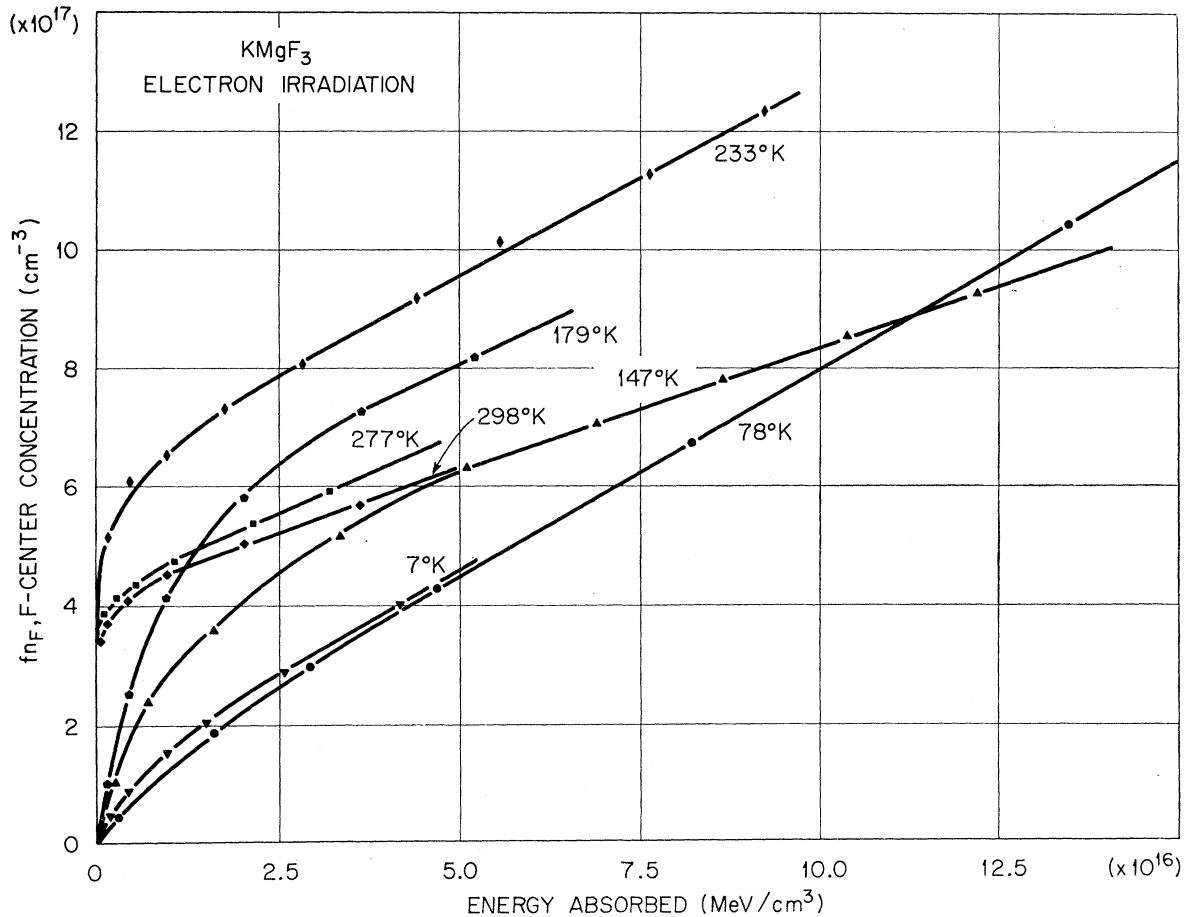


FIG. 11. Plot of the F -center concentration versus energy absorbed as a function of radiation temperature.

with this assignment. The annealing of this center for a warming rate of $4^\circ\text{K}/\text{min}$ is shown in Fig. 9. The dashed line is data for centers which had previously been oriented by a $[1\bar{1}0]$ bleach and then monitored with $[1\bar{1}0]$ light during the warmup. As can be seen, re-orientation occurs at about 95°K ; and there are annealing stages at 115 and 155°K .

Another band around 580 nm appears in irradiated crystals. From its radiation equilibrium relationship with the F band, its annealing characteristics, and some initial polarization data it appears that this band could be due to F_2^+ centers. However, sufficient evidence is not available to make a definite assignment at this time.

Defect Production

The intensity dependence of F -center production at 310°K is depicted in Fig. 10. The samples are impure enough (see Table I) that one might expect, in analogy with impurity-doped alkali halides, the late stage coloration to be completely suppressed for low radiation intensities. This seems to be the case. Figure 11 is a plot of the F -center concentration n_F times the oscillator

strength f of the F center versus absorbed energy dose as a function of radiation temperature for electron irradiated samples. The concentration of centers is related to the absorption coefficient at the peak of the band by Smakula's equation, which for a Gaussian band shape is

$$fn_F = 0.87 \times 10^{17} \mu_F (\mu_F^2 + 2)^{-2} W \alpha_F,$$

where $\mu_F = 1.35$ is the refractive index at 270 nm , and W is the half-width of the band. It should be noted that the efficiency of coloration increases with increasing radiation temperature up to about 233°K and then decreases. We also found that the ratio of F_2 centers to F centers remained statistical for radiation temperatures up to about 233°K , where some form of motion must occur so that relatively more F_2 centers are formed.

DISCUSSION AND SUMMARY

The location of the absorption bands due to F , F_2 , and V_K centers has now been well established by the work of Hall and the data presented here. It is interest-

TABLE II. Color centers in KMgF_3 and LiF .

| Center | KMgF_3 | | LiF^a | |
|--------|-----------------------------|-----------------------|-----------------------------|-----------------------|
| | Absorption energy [eV (nm)] | Huang-Rhys factor S | Absorption energy [eV (nm)] | Huang-Rhys factor S |
| F | 4.60 (270) | 75 | 5.00 (250) | 40 |
| F_2 | 2.78 (445) | 11 | 2.76 (450) | 8 |
| F_3 | 3.12 (395) | | 3.26 (380) | 3.9 |
| V_K | 3.65 (340) | | 3.55 (350) | |

^a Reference 8.

ing that the absorption bands of these defects in LiF , whose lattice constant is 4.0173 \AA , are very close to the same as for KMgF_3 , with a similar lattice constant of 3.973 \AA but with a different crystal structure. Table II shows a comparison of the band positions and Huang-Rhys factors for defects in these two types of crystals. If a linear coupling of the ground and excited states of a defect is assumed, then a knowledge of the peak position of the absorption, the Huang-Rhys factor, and the ground-state vibration frequency allows a prediction of the position of the luminescence band. Hall and Leggeat² have found the F_2 -center luminescence to occur at 2.19 eV (566 nm). In the case of linear coupling the peak positions of the absorption and emission of a defect are related by the equation $E_{\text{em}} = E_{\text{p}} - 2S\hbar\omega$. Therefore, we would predict F_2 -center emission to occur at 2.32 eV (534 nm).

The process of radiation damage in KMgF_3 is very similar to that in KCl . The dominant damage mechanism is apparently a photochemical one, since F centers can be readily produced with a production energy per F center far less than one would expect for elastic collision processes such as occur in MgO .¹⁰ The temperature dependence of the coloration process is also much like that in alkali halides, i.e., the efficiency for defect production becomes greater as the radiation temperature increases until temperatures in the range 200°K are reached at which time some type of "back reaction" occurs and the efficiency apparently decreases. Two explanations for this decrease in efficiency and for the strong dependence of the room-temperature colorability on radiation intensity and trace impurity content

¹⁰ W. A. Sibley and Y. Chen, *Phys. Rev.* **160**, 712 (1967).

have been proposed. Pooley¹¹ has suggested that the suppression of the colorability is due to a definite inhibition of the primary process of F -center production, which arises because impurities act as electron-hole recombination centers. It is his proposal that near an impurity, recombination of an electron-hole pair does not result in a replacement sequence and the formation of a vacancy-interstitial pair as it would if the electron and hole recombined in the perfect lattice. An alternate explanation¹² is that enhanced interstitial-vacancy recombination occurs because increased electron-hole recombination at impurities results in a greater concentration of mobile F^+ centers (α centers) than would be expected if recombination only occurred in the perfect lattice. Dawson and Pooley¹³ have demonstrated that in KI the first proposal is the most important. In this material the reduced colorability with increasing radiation temperature is due to a reduced formation rate of F centers. The evidence given in this paper, however, as can be clearly seen by a comparison of Figs. 5, 9, and 11, is that suppression of the colorability occurs at about the same temperature as the increased formation of F_2 centers and that both of these events happen at temperature much greater than that for which the V_K is mobile. Thus, in KMgF_3 it appears that the suppression of the colorability is associated with an enhanced destruction rate.

In summary, we may say that the absorption bands in KMgF_3 due to F , F_2 , F_3 , and V_K centers have been identified or substantiated and that in this material the enhanced recombination of vacancy-interstitial pairs due to vacancy mobility at high temperatures is more effective at suppressing the coloration than is an inhibition of the formation rate. The latter observation, when compared with the results of Dawson and Pooley, suggest that in all materials there is a competition between the two processes mentioned above with the latter process dominating in KI and the former in KMgF_3 .

¹¹ D. Pooley, *Proc. Phys. Soc. (London)* **87**, 257 (1966); **89**, 723 (1966).

¹² E. Sonder and W. A. Sibley, *Phys. Rev.* **129**, 1578 (1963); J. W. Mathews, W. C. Mallard, and W. A. Sibley, *ibid.* **146**, 611 (1966).

¹³ R. K. Dawson and D. Pooley, *Solid State Commun.* **7**, 1001 (1969).